JOURNAL OF MATERIALS SCIENCE 25 (1990) 2869–2872

Nonlinear constitutive equation of polypropylene under combined tension and torsion

M. KITAGAWA, H. TAKAGI
Department of Mechanical Engineering, Faculty of Technology, Kanazawa University, Kanazawa, Japan

Combined tension and torsion tests were performed at various strain histories using polypropylene (PP) hollow cylinders. The experimental stress–strain curves were compared with the multiaxial constitutive equation which is extended from the uniaxial one based on the overstress concept of Krempl. It is shown that the theory agrees with the experimental curves under pure torsion as well as combined tension–torsion, provided that the current strain is not below the maximum strain.

1. Introduction

Although much effort has been made to introduce a nonlinearity in the linear theory of viscoelasticity, the nonlinear behaviour at finite strains are less understood because of the many complexities peculiar to polymer solids.

In previous papers, the experimental stress–strain curves under uniaxial compression [1] and pure torsion [2] were compared with the numerical results derived from a uniaxial nonlinear theory based on an overstress concept proposed by Krempl [3, 4]. It is shown that the overstress theory agrees with the experimental data under constant strain rate, stress relaxation, sudden change of strain rate, creep and combined states of them, provided that the current strain is not below the maximum strain. Hence, the uniaxial overstress theory may be concluded to be useful for inferring a uniaxial stress–strain behaviour of strongly time-dependent solids like polymers at finite strains.

The purposes of this paper are to give some experimental stress–strain curves under biaxial stress states and to compare the experimental data with a multiaxial constitutive model extended from the uniaxial equation. For these purposes, combined tension–torsion tests were executed at various strain histories.

2. Experimental details

The material used was extruded rods of commercial polypropylene (PP). Hollow cylindrical specimens with outer and inner diameters of 16 mm and 12 mm and a gauge length of 21 mm were machined from them for combined tension and torsion stressing. After machining, they were annealed for 2 h at 70° C.

A home-made servocontrolled machine, which was used in the previous report, was prepared for the tests. The test results were recorded on a microcomputer.

Tests were performed under constant strain rate, sudden change in strain rate and stress relaxation. All tests were executed at room temperature. The true stress σ (applied load/current cross-sectional area) and the logarithmic strain ε were used for tension. The torsional stress τ and the engineering shear strain γ defined as

$$\tau = T/\{\pi(d_0^2 - d_1^2)/4 \cdot (d_0 + d_1)/2\}$$
$$\gamma = (d_0 + d_1)/2 \cdot \theta/L \quad (1)$$

are used where T is the applied torque, θ is the twist angle over the specimen gauge length L, and d_0 and d_1 are the outer and the inner specimen diameters, respectively.

In the tensile strain ranges higher than about 0.1, a few crazes were observed along the specimen axis. But an increase in tensile strain due to crazing may be regarded as small. In this paper, therefore, the effect of these crazes on the stress–strain curve was not considered.

In some graphs a schematic diagram is illustrated to facilitate the interpretation of the loading path.

3. Test results and discussions

3.1. Extension of uniaxial to multiaxial constitutive model

The previous papers [1, 2] showed that an overstress theory explains the uniaxial stress–strain curves of PP at constant strain rate, sudden change in strain rate, stress relaxation and creep.

The governing equation of the overstress theory is given for torsion by

$$K\dot{\tau} + \tau = M\dot{\gamma} + g[\gamma]$$
$$K = K[\tau - g[\gamma], \gamma], \quad M/K = G \quad (2)$$

where $g[\gamma]$ is an equilibrium stress–strain curve obtained at a strain rate of $\dot{\gamma} = 0$, G is the elastic shear modulus, the dot denotes the differentiation with respect to time and the bracket $[\cdot]$ means the function of the argument. The quantity $\tau - g[\gamma]$, the deviation

0022–2461/90 $03.00 + .12

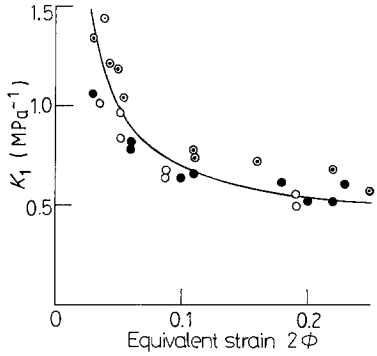

Figure 1 Comparison of K_1 function in Equation 3 between compression and torsion: (○) compression, [1], (●) torsion; and (◉) torsion [2]. The solid curve shows Equation 3 with the constants given in Equation 5.

of the current stress τ from the equilibrium value at γ, is called an overstress. The K function can be determined empirically. The method for deciding the K function is described in detail in [1, 2]. The K function can be approximated by

$$K = K_0 \exp\{-K_1[\gamma](\tau - g[\gamma])\}$$
$$K_1[\gamma] = P_0 + P_1/\gamma \quad (3)$$

Equation 3 is slightly different from the previously used one denoted by $K_1 = P_0 + P_1/(P_2 + \gamma)$. But the value of P_2 was chosen to be very small in the previous papers [1, 2] and therefore, this term is ignored in this article.

For PP which shows a slight work softening at high strain regions, $g[\gamma]$ is well described as

$$g[\gamma] = (g_m/f)\{\tanh(b\gamma/\gamma_m) - (\operatorname{sech} b_0)^2(b\gamma/\gamma_m)\}$$
$$f = b_0(\tanh b_0)^2 + \tanh b_0 - b_0$$
$$b = b_1 + b_2 - b_2 \exp(-b_3\gamma)$$
$$b_1 = f\gamma_m G/\{(\tanh b_0)^2 g_m\}$$
$$b_2 = 2b_0 - b_1 \quad (4)$$

where g_m is the maximum stress in the equilibrium curve, and b_0, b_3 and γ_m are constants selected to fit the experimental data.

The computed results of Equation 2 have proved to agree with the experimental data [1, 2]. The constants

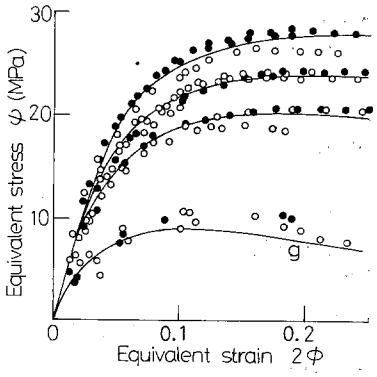

Figure 2 Equivalent stress ψ–equivalent strain ϕ curves obtained at compression and torsion tests performed at different strain rates of about $2\dot{\phi} = 1.4 \times 10^{-4}$, 1.4×10^{-3} and $1.4 \times 10^{-2}\,sec^{-1}$. The solid and the open circles denote the compression and torsion data, respectively. The solid surves are theoretical. The circles near the curve g are the relaxation limits which would be achieved at 24 h relaxation tests.

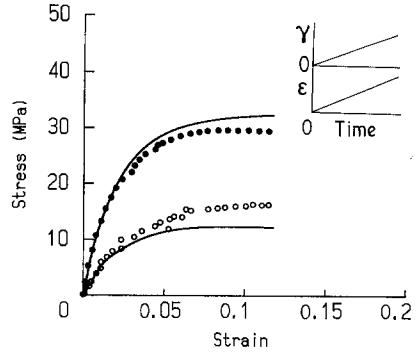

Figure 3 Stress–strain curves under combined tension–torsion loading: $\dot{\varepsilon} = 0.64 \times 10^{-3}\,sec^{-1}$, $\dot{\gamma} = 0.36 \times 10^{-3}\,sec^{-1}$. The solid circles show tensile (σ–ε) data and the open circles torsional (τ–γ) data. The solid curves are theoretical.

used for the calculations are

$$G = 490\,MPa, \quad g_m = 8.82\,MPa, \quad \gamma_m = 0.21$$
$$b_0 = 2.0, \quad b_3 = 80$$
$$K_0 = 7.94 \times 10^4\,sec$$
$$P_0 = 0.39\,MPa^{-1}, \quad P_1 = 0.31\,MPa^{-1} \quad (5)$$

These are slightly different from the previous values.

Here, we try to develop the uniaxial constitutive Equation 2 to a multiaxial model.

According to the experimental measurement of change in specimen volume during compression, the volume expansion is reported to be regarded as considerably smaller than the compressive strain. The ratio of the volume expansion to the compressive strain is only about 1/30 [5]. Hence, in this paper, we assume that the material used is incompressible. In an isotropic material, the uniaxial constitutive Equation 2 may be naturally extended to the multiaxial one given as

$$K\dot{S}_{IJ} + S_{IJ} = M\dot{e}_{IJ} + g_{IJ}$$
$$K = K_0 \exp(-K_1[\phi]\zeta), \quad M/K = G$$
$$K_1[\phi] = P_0 + P_1/(2\phi)$$
$$g_{IJ} = e_{IJ}\, g_e[\phi]/\phi$$
$$g_e[\phi] = g[2\phi]$$
$$\phi = (e_{IJ}\, e_{IJ}/2)^{1/2}$$
$$\zeta = \{(S_{IJ} - g_{IJ})(S_{IJ} - g_{IJ})/2\}^{1/2} \quad (6)$$

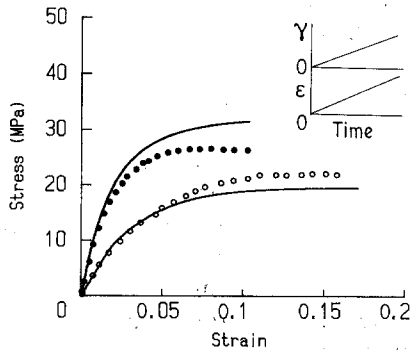

Figure 4 Stress–strain curves under combined tension–torsion loading: $\dot{\varepsilon} = 0.44 \times 10^{-2}\,sec^{-1}$, $\dot{\gamma} = 1.04 \times 10^{-2}\,sec^{-1}$. The solid circles show tensile (σ–ε) data and the open circles torsional (τ–γ) data. The solid curves are theortical

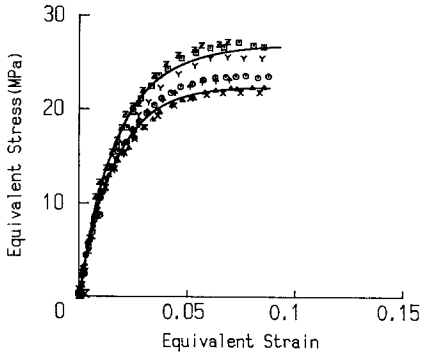

Figure 5 Equivalent stress ψ–equivalent strain ϕ curves at constant strain rates under combined tension–torsion stressings, (Y) $\dot{\phi} = 0.58 \times 10^{-2}\,\text{sec}^{-1}$, $R\,(=\dot{\gamma}/3^{1/2}\dot{\varepsilon}) = 0.32$, (Z) $\dot{\phi} = 0.5 \times 10^{-2}\,\text{sec}^{-1}$, $R = 0$, (□); $\dot{\phi} = 0.57 \times 10^{-2}\,\text{sec}^{-1}$, $R = 1.05$; (△) $\dot{\phi} = 0.46 \times 10^{-3}\,\text{sec}^{-1}$, $R = \infty$; (X) $\dot{\phi} = 0.6 \times 10^{-3}\,\text{sec}^{-1}$, $R = 0$; and (▲) $\dot{\phi} = 0.59 \times 10^{-3}\,\text{sec}^{-1}$, $R = 0.45$. The solid curves are theoretical (tension–torsion at $\dot{\phi} = 0.57 \times 10^{-2}\,\text{sec}^{-1}$ and tension at $\dot{\phi} = 0.6 \times 10^{-3}\,\text{sec}^{-1}$).

where S_{IJ} and e_{IJ} are the deviative stress and strain tensors, $g[\gamma = 2\phi]$ is the quilibrium stress–strain curve defined in Equation 4. ϕ is the equivalent strain and ζ is the equivalent overstress. The similar equation has been proposed by Cernocky and Krempl [6] for the material of which dilative strain is comparatively large and then cannot be ignored.

The assumption that the material is incompressible may lead to

$$(3/2)(M/K) = 3G = E \tag{7}$$

where E is the elastic modulus.

Under a combined tension (σ, ε) and torsion (τ, γ) state, Equation 6 may be simplified to

$$\begin{aligned} K\dot{\sigma} + \sigma &= (3/2)M\dot{\varepsilon} + (3/2)\,\varepsilon\, g[2\phi]/\phi \\ K\dot{\tau} + \tau &= M\dot{\gamma}/2 + \gamma\, g[2\phi]/(2\phi) \\ \phi &= (3\varepsilon^2 + \gamma^2)^{1/2}/2 \\ \zeta &= \{3(2\sigma/3 - \varepsilon g[\phi]/\phi - \varepsilon g[\phi]/\phi)^2 \\ &\quad + 4\,(\tau - \gamma g[\phi]/2\phi)^2\}^{1/2}/2 \end{aligned} \tag{8}$$

where γ is the engineering shear strain. For pure torsion, Equation 8 may reduce to Equation 2 if M in Equation 8 is replaced by $2M$.

The slopes on a log K–ζ diagram determined empirically are shown against the equivalent strain

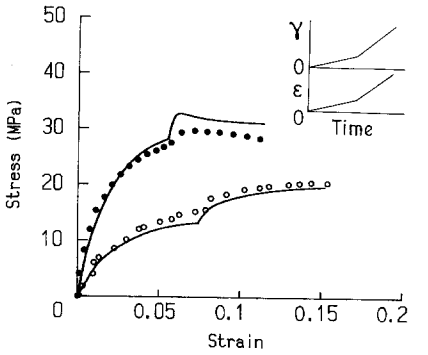

Figure 6 Stress–strain curves with sudden increase in strain rate under combined tension–torsion loading: $\dot{\varepsilon} = 0.38 \times 10^{-3}\,\text{sec}^{-1}$, $\dot{\gamma} = 0.54 \times 10^{-3}\,\text{sec}^{-1} \rightarrow \dot{\varepsilon} = 0.43 \times 10^{-2}\,\text{sec}^{-1}$, $\dot{\gamma} = 0.96 \times 10^{-2}\,\text{sec}^{-1}$. The solid circles show tensile (σ–ε) data and the open circles torsional (τ–γ) data. The solid curves are theoretical.

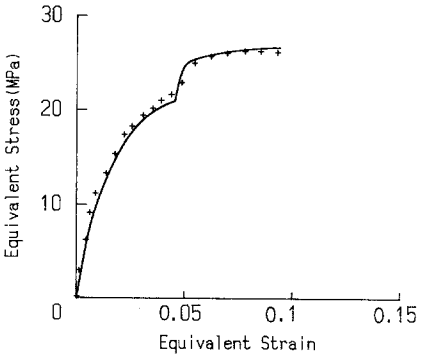

Figure 7 Replot of Fig. 6 on an equivalent stress ψ–equivalent strain ϕ diagram. The solid curve is theoretical.

for both pure torsion and uniaxial compression in Fig. 1. The solid curves show Equations 2 to 6 with the constants given by Equation 5. The results reveal that the K function is independent of the loading method and the functional form mentioned above is suitable.

It is to be noted that when a tensile test is performed at $\dot{\varepsilon} = \dot{\gamma}/3^{1/2}$, the tensile stress–strain curve described on a $\sigma/3^{1/2}$–$3^{1/2}\,\varepsilon$ diagram is identical to the torsional τ–γ curve.

This can be confirmed in Fig. 2 where the stress–strain curves obtained at different equivalent strain rates $\dot{\phi}$ for both compression and torsion are plotted in a ψ–ϕ diagram. The circles near the curve g show the relaxation limits. The equivalent strain rate $\dot{\phi}$ and the equivalent stress ψ are defined for a combined tension–torsion state as

$$\dot{\phi} = (3\dot{\varepsilon}^2 + \dot{\gamma}^2)^{1/2}/2 \tag{9}$$

$$\psi = (\sigma^2/3 + \tau^2)^{1/2} \tag{10}$$

This may provide evidence that the constitutive Equation 8 is valid for the material PP used here.

3.2. Comparison of Equation 8 with experimental data

The biaxial constitutive Equation 8 is compared with the stress–strain curves under combined tension–torsion stressing. The experimental data recorded on the microcomputer are plotted without modification, and then are slightly scattered in the figures described later.

The experimental data obtained at equivalent strain rates $\dot{\phi} = 0.64 \times 10^{-3}$ and $0.57 \times 10^{-2}\,\text{sec}^{-1}$ are

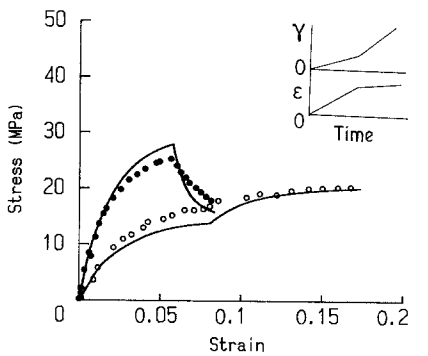

Figure 8 Stress–strain curves with sudden change in strain rate under combined tension–torsion loading: $\dot{\varepsilon} = 0.39 \times 10^{-3}\,\text{sec}^{-1}$, $\dot{\gamma} = 0.6 \times 10^{-3}\,\text{sec}^{-1} \rightarrow \dot{\varepsilon} = 0.16 \times 10^{-3}\,\text{sec}^{-1}$, $\dot{\gamma} = 1.02 \times 10^{-3}\,\text{sec}^{-1}$. The solid circles show tensile (σ–ε) data and the open circles torsional (τ–γ) data. The solid curves are theoretical.

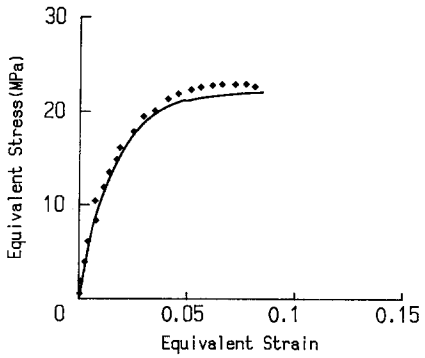

Figure 9 Replot of Fig. 8 on an equivalent stress ψ–equivalent strain ϕ diagram. The solid curve is theoretical.

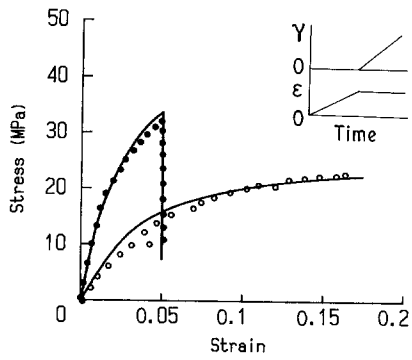

Figure 10 Stress–strain curves with sudden change in strain rate under combined tension–torsion loading: $\dot{\varepsilon} = 0.54 \times 10^{-3}\,\mathrm{sec}^{-1}$, $\dot{\gamma} = 0\,\mathrm{sec}^{-1} \rightarrow \dot{\varepsilon} = 0\,\mathrm{sec}^{-1}$, $\dot{\gamma} = 1.76 \times 10^{-3}\,\mathrm{sec}^{-1}$. The solid circles show tensile (σ–ε) data and the open circles torsional (τ–γ) data. The solid curves are theoretical.

shown by the circles in Figs 3 and 4 where the details of loading path are also denoted. The solid curves are drawn based on the numerical calculation of Equation 8 with the constants given in Equation 5.

The curves in Figs 3 and 4 are replotted on a ψ–ϕ diagram in Fig. 5 where the other data tested at constant strain rate $\dot{\phi}$ with different strain rate ratios of $R = \dot{\gamma}/(3^{1/2}\,\dot{\varepsilon})$ are also shown. $R = 0$ means a pure torsion, while $R = \infty$ denotes a uniaxial tension. It may be shown that the ψ–ϕ data obtained at the same equivalent strain rate construct the same curve independent of the ratio R. The theoretical curves (solid lines) trace the experimental data well.

Figure 6 denotes the results with sudden change in strain rate. A specimen was loaded at a certain rate to a predetermined strain, and then the strain rate was suddenly increased by an order of magnitude. The results in Fig. 6 are denoted on a ψ–ϕ diagram in Fig. 7, where the solid curves are theoretical. The experimental data show an elastic response immediately after the strain rate change and then gradually approach the stress–strain behaviour expected at the new rate. The calculated results agree with this trend.

Figure 8 shows the case where the strain rate ratio R was changed from $R = 0.89$ to $R = 3.68$ during the test, the equivalent strain rate $\dot{\phi}$ being kept nearly constant. Fig. 9 shows the replot of the data of Fig. 8. If the equivalent strain rate $\dot{\phi}$ is kept constant, the curve becomes coincident with the one expected at the same equivalent strain rate, whatever value the initial strain ratio R is changed to during the test. The theory drawn by the solid curve agrees with the experimental result.

Initially tensile loading was applied at a constant strain rate up to a predetermined strain, while torsional torque remains free. After the tensile strain amounted to the predetermined one, the torsion test started at a constant strain rate, the tensile strain being kept constant. The input strain function is schematically illustrated in Fig. 10. The experimental result for this strain history is shown in the figure. The theory denoted by the solid curves agrees with the trend that the stress relaxation occurs in an abrupt manner as soon as the torque begins to increase.

All the results show that the biaxial constitutive equation proposed here is useful for a viscoelastic-plastic material like PP which may be regarded as incompressible.

In this paper, the case where the equivalent strain ϕ becomes less than the maximum strain has not been reported. In that case, the theory proposed here should be somewhat modified. A new constitutive equation including the reversed loading path, which may be developed from the above mentioned concept, will be reported in future.

Acknowledgement

The authors wish to thank Mr K. Mizutani for his experimental assistance.

References

1. M. KITAGAWA and T. MATSUTANI, *J. Mater. Sci.* **23** (1988) 4085.
2. M. KITAGAWA, T. MORI and T. MATSUTANI, *J. Polymer Sci. Part B. Polymer Physics* **27** (1989) 85.
3. E. KREMPL, Trans. ASME, *J. Eng. Mater. Tech.* **101** (1979) 380.
4. M. C. LIU and E. KREMPL, *J. Mech. Phys. Solids* **27** (1979) 377.
5. M. KITAGAWA and T. YONEYAMA, *J. Polym. Sci., Part C* **26** (1988) 207.
6. E. P. CERNOCKY and E. KREMPL, *Int. J. Solids Structures* **16** (1980) 723.

Received 24 January
and accepted 24 August 1989